JOURNAL OF CATALYSIS **161,** 500–506 (1996)
ARTICLE NO. 0211

The Influence of Support on the Low-Temperature Activity of Pd in the Reaction of CO Oxidation

1. The Structure of Supported Pd

D. I. Kochubey, S. N. Pavlova, B. N. Novgorodov, G. N. Kryukova, and V. A. Sadykov

Boreskov Institute of Catalysis, Siberian Branch of the Russian Academy of Sciences, Novosibirsk, Russia

Received March 21, 1994; revised October 27, 1995; accepted January 24, 1996

The morphology of small Pd clusters on SiO_2, TiO_2, and Al_2O_3 and the influence of CO and the reaction mixture $CO + O_2$ on their fine structure have been investigated by TEM and EXAFS. For all supports, Pd particles have a quite narrow size distribution with mean diameters in the range 15–25 Å, whereas their morphology and spatial homogeneity of location on the support are different. EXAFS data acquired in controlled-atmosphere cells have shown distortion of Pd surface layers to depend upon the nature of the support and/or the adsorbate. Disordering of Pd surface structure suggests appearance of the defect centers of CO and oxygen adsorption.

INTRODUCTION

At temperatures higher than 400 K the reaction of carbon monoxide catalytic oxidation is known to be structure insensitive; i.e., turnover numbers are independent of the surface orientation of Pd single crystals and the sizes of supported particles (1–3). However, at ambient temperatures, supported Pd is very active in this reaction (4–7), while bulk metal is practically inactive (8). Thus, a question arises about the nature of the support influence, which could manifest itself in phenomena such as decoration of the metal particles by support species, chemical modification, support-induced morphological and structural changes, generation of reactive species adsorbed on the support or at the metal/support interface, and spillover. Apart from its theoretical significance (9, 10), the question has considerable practical importance since in monolith catalysts for automotive control, Pd provides high activity under cold-start conditions (8). Therefore, the necessity of complex investigation of the structural, adsorption, and catalytic properties of supported catalysts to elucidate the nature of the low-temperature activity of supported Pd seems obvious.

In pursuing these aims we have investigated Pd supported on the most widely used carriers such as SiO_2, TiO_2, and γ-Al_2O_3. The first article of this series is devoted to the EXAFS and TEM study of the structure and morphology of small Pd particles. Inasmuch as one of the possible reasons for high activity of supported Pd is rearrangement of its structure induced by the reaction mixture (11), EXAFS cells with controlled atmospheres were used in the experiments.

EXPERIMENTAL

Three types of supports were used in this work: TiO_2 (anatase), $S_{sp.} = 100$ m^2/g; γ-Al_2O_3, $S_{sp.} = 180$ m^2/g; SiO_2, $S_{sp.} = 300$ m^2/g. The catalysts were prepared in an all-glass setup without air contact. The samples of the support (fraction 0.25–1 mm) were evacuated at 673–743 K (ca. 10^{-1} Torr) for 4 h. The pretreated supports were wetted with benzene and then impregnated with $Pd(OAc)_2$ solution in the same solvent. After salt adsorption, the excess solution was decanted and the catalyst was dried under vacuum at 353 K for 1 h. Prepared catalysts were kept under air and were reduced in H_2 flow immediately before experiments at 673 K (Pd/SiO_2 and Pd/Al_2O_3) or 743 K (Pd/TiO_2). Pd content in all catalysts was nearly identical: 2.47% Pd/SiO_2, 2.6% Pd/Al_2O_3, and 2.3% Pd/TiO_2.

For EXAFS experiments, vacuum-tight cells specially designed by the authors and manufactured at the Boreskov Institute of Catalysis have been used. These cells are assembled from stainless-steel rings and 200 μm thick beryllium windows hermetically joined by diffusion welding. To ensure an optimum absorption jump (usually ca. 0.8–1.0) at the K edge of Pd, a set of cells with thickness varying from 2 to 10 mm was used to adjust a sample amount. Two holes in the ring made it possible to fill in or discharge the powdered catalysts (ca. 0.1 mm fraction) via welded Fernico tubes sealed to the glass tubes. If the glass tubes are sealed off, the cell is vacuum-tight (gas leakage is less than 10^{-3} Torr per week). To eliminate any gas desorption from walls of the cell, it was preannealed at 673 K under continuous pumping.

0021-9517/96 $18.00

Before the sample pretreatment, the EXAFS cell was sealed to the glass-made catalytic reactor so that the gas-phase composition was identical in both parts of the setup. After pretreatment, the catalyst was poured out of the reactor into the cell via tubes without any air contact. Then the glass tubes were sealed off, keeping the atmosphere in the cell intact, and such hermetically isolated samples were studied in the EXAFS experiments.

Three series of measurements were conducted.

Series A. The catalysts were placed in the reactor with a sealed EXAFS cell and reduced in a 30 cm^3/min H_2 flow for 1 h at 673 or 743 K. Following reduction, this setup was evacuated for 30 min at the reduction temperature and at a pressure of 10^{-3} Torr. The sample was then cooled to room temperature while still under vacuum and poured out of the reactor into the cell as described above.

Series B. The catalyst pretreatment was conducted similarly to that of Series A up to the pouring out procedure. Thereafter the setup was purged by a mixture of 1% CO in He (30 cm^3/min.) for 15 min at 298 K. The catalyst was then poured out of the reactor into the cell without evacuation.

Series C. The procedure was identical to that of Series B except that the 1% CO + 19% O_2 mixture was passed through the catalyst for 3 h at 298 K with subsequent evacuation for 5 min to remove the gas phase. The catalyst was then poured out of the reactor into the cell while still under vacuum.

EXAFS spectra of the *K* edge of palladium X-ray absorption were obtained at the EXAFS Station of the Siberian Center of Synchrotron Radiation, Novosibirsk (12). The storage ring VEPP-3 with electron beam energy 2 GeV and a typical filled current of 70 mA was used as the radiation source. The energy of the synchrotron radiation quanta was monitored with the help of the cutoff Si(111) monochromator. The higher harmonics (3 $h\nu$, etc.) for the energies around the Pd *K* edge (24.6 keV) were found to be absent in the spectra of the VEPP-3 radiation source. X-ray absorption spectra were recorded in the transmission mode using two ionization chambers, i.e., the monitoring chamber and the full absorption chamber. The monitoring chamber contained 0.5 atm of Ar and was located in front of the sample, while the full absorption chamber contained 1 atm of Xe and was located behind the sample. Solid PdO and $Pd(OAc)_2$ with the known structures were used to calibrate the phase correction δ for Pd–*L* distance, where *L* is the oxygen or carbon atom of a ligand in the first coordination shell of the metal atom. These reference samples of special pure grade were especially prepared and tested by X-ray diffraction.

For each sample, X-ray absorption data were analyzed for interval of the wave numbers *k* from 3.0 to 14.0 $Å^{-1}$ in the form of $k\chi(k)$ and $k^3\chi(k)$, where $\chi(k)$ is the oscillating part of the absorption coefficient μ. The background was removed by extrapolating absorption in the preedge region onto the EXAFS region in the form of Victoreen's polynomials. Three cubic splines were used to construct the smooth part of μ. The inflection point of the edge of the X-ray absorption spectrum was used as the initial point ($k = 0$) of the EXAFS spectrum. The RDA function was calculated from the EXAFS spectra in $k\chi(k)$ or $k^3\chi(k)$ forms using Fourier analysis (12) and comparison with the RDA curve of a Pd foil. An alternative curve fitting with the help of the EXCURVE-92 (a commercial program distributed by BioSim) procedure was also used to determine interatomic distances from the EXAFS spectra. Whenever both procedures were applied to the same EXAFS spectrum, they gave very similar values for the same Pd–Pd and Pd–*L* distances. For the same sample and the same procedure of analysis (Fourier analysis or fitting), very close values of Pd–Pd and Pd–ligand distances were obtained from EXAFS spectra in $k\chi(k)$ and $k^3\chi(k)$ forms. The phase correction δ for Pd–Pd and Pd–*L* distances for a given interval of *k* values, which has to be known when one looks for Pd–Pd and Pd–*L* distances from RDA curves obtained via Fourier analysis, was found experimentally from RDA curves for the reference materials, i.e., Pd foil with the known Pd–Pd distances and the complex PdO with a known structure.

The initial analysis methods listed here were found to be unsatisfactory for the needs of this study. Hence, to describe adequately the distribution of Pd atoms in clusters around a mean position, the authors were forced to elaborate an original approach based upon estimation of the validity of the Debye–Waller approximation as in (13) (*vide infra*).

The catalysts of Series A were examined in a JEM-100 CX electron microscope in the bright-field mode. The resolution limit of the machine was ca. 3Å; the accelerating potential was 100 kV. The samples for investigation were prepared from a suspension in ethanol with subsequent support on perforated carbon films mounted on copper grids.

RESULTS

TEM

For all samples the Pd particles have a quite narrow size distribution (Fig. 1). The mean diameters derived from histograms and those calculated from the oxygen chemisorption data are given in Table 1. The Pd particles on SiO_2 (Fig. 2a) are uniformly distributed on the support. The shape of the particles is nearly spherical, the clusters being "elevated" over the surface of the support and connected with it by a sort of fibers. The analogous type of bonding was observed earlier (14) for Pt on SiO_2. The observed phenomena could arise from the migration of SiOH groups under the action of water vapor formed in the course of reduction of the oxidized forms of Pd.

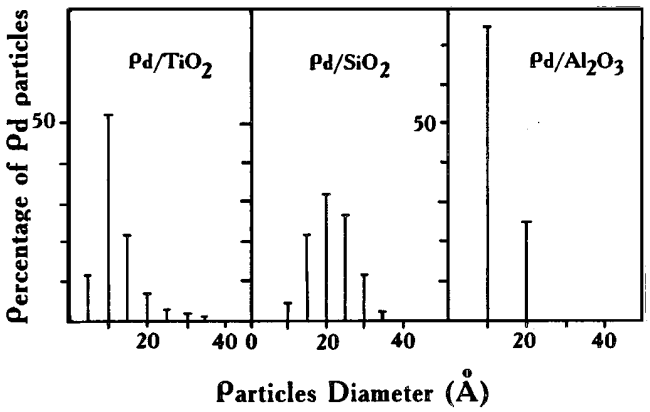

FIG. 1. The size distribution of Pd particles on different supports.

As in the case of Pd/SiO_2, the distribution of the palladium particles on TiO_2 is also uniform, but with the clusters flattened (Fig. 2b). They are fixed on the most developed (110) faces of the well-crystallized platelets of anatase. For this face the distance between the regular Ti cation and the nearest empty interstices is close to 2.6 Å, that is, not very different from the Pd–Pd distance in supported clusters. Such matching of the structures could favor a metal–support interaction. Figure 2c demonstrates a nonuniform distribution of the Pd particles on the surface of γ-Al_2O_3: rather large areas are free from the metal clusters. In this case metal particles have no preferential forms and are predominantly fixed on such defects of the support as steps and kinks.

EXAFS

For all samples studied here, RDA curves were found to be identical. To demonstrate the quality of the original experimental data in $k\chi(k)$ presentation as well as the coincidence of the RDA curves for Pd foil and catalysts, the data for Pd/TiO_2 are plotted in Fig. 3.

According to EXAFS data (Table 2), for all Series A samples Pd is completely reduced to metallic state. In all cases the first Pd–Pd distance somewhat differs from that for Pd foil (up to 0.08 Å), the deviation being dependent upon the nature of the support. The increase of the σ^2 Debye factor (up to 0.003 $Å^2$) relative to foil was also observed for supported Pd, indicating the structure of small particles to be disordered.

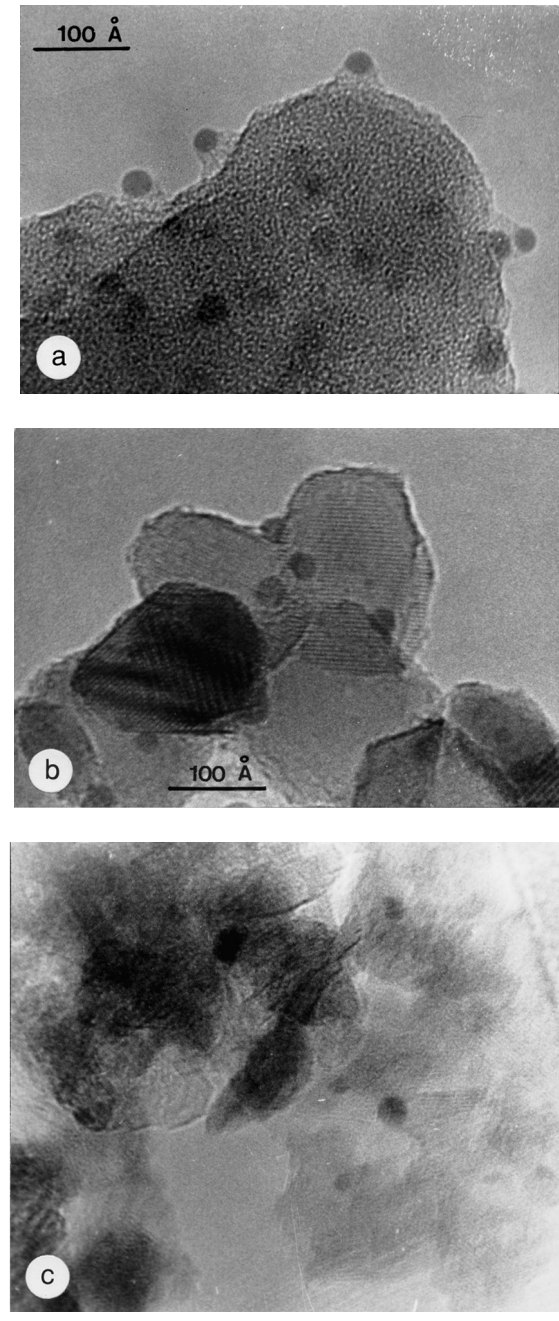

FIG. 2. Bright-field electron micrographs: (a) Pd/SiO_2; (b) Pd/TiO_2; (c) Pd/Al_2O_3.

TABLE 1

Mean Pd Particle Diameters

Sample	Treatment	Mean particle diameter (Å)		S_{Pd}, m^2/g_{Pd}
		O_2 chem.	TEM	
2.3% Pd/TiO_2	743 K, H_2	18	15.6	268
2.47% Pd/SiO_2	673 K, H_2	18	24	174
2.6% Pd/Al_2O_3	673 K, H_2	15	15.7	266

Too low coordination numbers (N) for the Pd–Pd distance in small Pd clusters obtained from standard EXCURVE procedure (Table 2) are also worth mentioning. For Pd particles with typical size ca. 15 Å, the mean coordination number is commonly expected to be ca. 9, depending upon the particles' shape (15). We suggest that in our case underestimated coordination numbers are due to

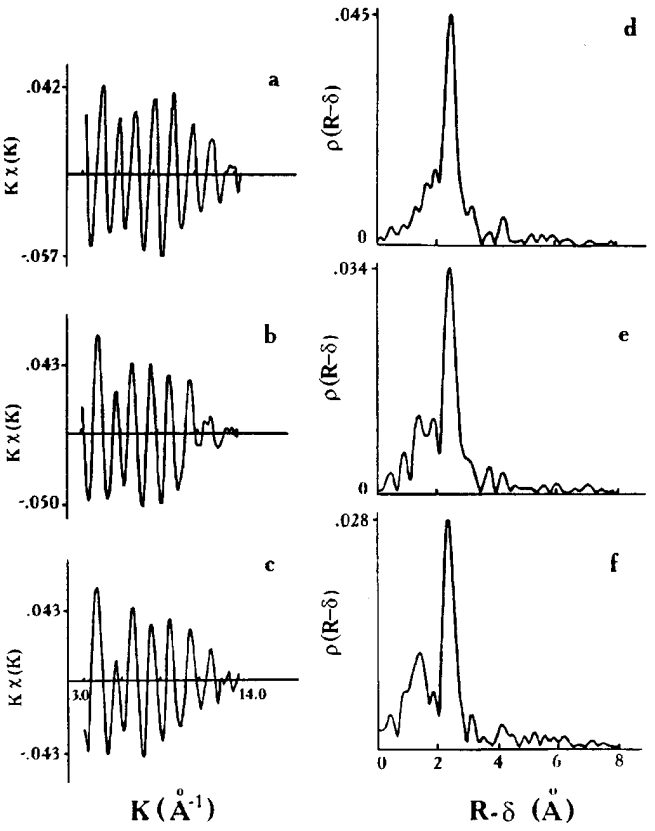

FIG. 3. EXAFS spectra $k\chi(k)$ and Fourier transforms $\rho(R-\delta)$ of the Pd/TiO_2 catalysts: (a, d) in vacuum; (b, e) in the atmosphere of CO; (c, f) in the reaction mixture.

improper choice of the structural model for Pd particles. Some arguments in favor of this assumption are as follows.

EXAFS oscillations are well known to be described by a model based upon approximation of the electron elastic scattering after one-electron photoionization, assuming Gaussian distribution of the interatomic distances around mean values (12). Restrictions caused by considering only elastic scattering are overcome by introduction of a photoelectron mean free path λ depending upon the wave vector k (usually $\lambda \sim 1/k$). The coefficient of the EXAFS oscillations allows one to cope with the limitations imposed by considering only one-electron excitations. It is well known also that that theory, which has no inelastic losses, overestimates the observed EXAFS. This factor is included in EXCURVE as a proportional multiplier S_0. Commonly S_0 is equal to 0.7–0.8 and is assumed to be similar in bulk metal and clusters. In most cases, Gaussian distribution makes it reasonably possible to take thermal vibrations of the lattice atoms into account. However, for real system, the interatomic distance distribution deviates from the Gaussian type due to disordering or proximity of the phase boundary. The same effects appear for structures with reduced symmetry. The impact of these deviations on the EXAFS parameters has already been considered, though without any analysis of the detailed mechanisms of this phenomenon. Due to these effects, either the coordination number drops or the maximum of the RDA curve is shifted (13).

At present, specific models of structures with a non-Gaussian distribution, together with analysis of the reasons for their appearance, have been considered in a number of papers (13, 16–18). First, there are structures in which temperatures of a phase transition are close to temperatures of the EXAFS measurements. In this case the potential well for the positioning of atom in the lattice (and the corresponding distribution of the thermal vibrations) becomes asymmetric. Second, there are structures wherein two or more types of scattering atoms situated in identical positions contribute to the same RDA curve peak (structures of an α-As_2S_3 type (16)). Peak positions can coincide even for differing interatomic distances if phase shift values compensate for such differences (17). Finally, there are structures wherein a set of interatomic distances are merged into one peak due to insufficient resolution of the EXAFS (18). This phenomenon occurs only if the number of parameters describing a RDA curve peak is too large to be analyzed by a conventional curve-fitting analysis, which is the case for MoO_3 (18).

We believe that the model of (17) is hardly probable here and does not agree with the results of other physical methods for the catalysts studied. In our opinion, for supported catalysts the most adequate models are based on structures where for some reason mean interatomic distances are not constant. At present it seems rather difficult (if even possible) to elaborate a complex model in which several operating factors such as amorphization, epitaxy, and point defects can be simultaneously taken into account. Since we are mainly interested in elucidating the factors that govern the catalytic activity of supported Pd, our attention was focused on the well-known phenomena of metal surface layer reconstruction leading to variation of the interatomic distances (19). Hence, as a first approximation, we can describe the structure of Pd particles as bimodal: the bulk structure is mainly a function of dispersion, while the surface part strongly depends upon the gases adsorbed. The contribution from each component strongly depends upon the particle sizes and morphology.

In the framework of this model, we have elaborated a curve-fitting procedure complementary to the routine analysis (12). To reduce the number of independent parameters and to check if the new structural model is indeed useful, a new strategy was chosen. Only two mean distances (one for the bulk and one for the surface layer) were assumed to exist, that for the surface being shorter due to the well-known phenomenon of surface contraction (19–21).

Along with Debye factor determination by a curve-fitting method, a procedure is known in which the dependence of $\ln[\chi_{exp}/\chi_{mod}]$ versus k^2 is constructed for one

TABLE 2

EXAFS Parameters of Supported Pd Catalysts

Sample	Treatment	Peak position $R-\delta$, Å	Peak intensity I	Interatomic distance R^a, Å	Coord. number, N^a	Debye–Waller factor σ^2, Å^2	Peak relation	ΔR, Å
Pd foil		2.44	0.080	2.74	12.0		Pd–Pd	
PdO		1.50	0.036	2.04	4.0	0.0052	Pd–O	
		2.89	0.030	3.04	4.2		Pd–Pd	
$Pd(Ac)_2$		1.55	0.043	2.06	4.5		Pd–O	
		2.66	0.014	3.01	1.2	0.0040	Pd–Pd	
Pd/SiO_2	Vacuum	2.51	0.044	2.81	7.1	0.0030	Pd–Pd	0.07
	CO	2.44	0.031	2.74	5.2	0.0044	Pd–Pd	0.03
	$CO + O_2$	1.48	0.017	2.02	1.5		Pd–O	
		2.57	0.024	2.87	4.1	0.0032	Pd–Pd	0.11
Pd/TiO_2	Vacuum	2.40	0.043	2.70	7.0	0.0024	Pd–Pd	0.05
	CO	2.40	0.032	2.70	6.8	0.0051	Pd–Pd	0.03
	$CO + O_2$	2.36	0.027	2.64	4.0	0.0036	Pd–Pd	0.08
Pd/Al_2O_3	Vacuum	2.36	0.031	2.64	5.2	0.0027	Pd–Pd	0.04
	CO	1.36	0.010	1.92	0.9		Pd–C	
		2.45	0.031	2.74	5.1	0.0024	Pd–Pd	0.02
	$CO + O_2$	1.50	0.018	2.04	1.6		Pd–O	
		2.27	0.014	2.66	3.2	0.0043	Pd–Pd	0.09

[a] Parameters calculated by the EXCURVE procedure. Uncertainty limits are R, 1%; N, 10%; σ^2, 40%.

coordination sphere extracted by Fourier transformation. According to the main formalism of EXAFS $\ln[\chi_{exp}/\chi_{mod}] = -2(\sigma^2_{exp} - \sigma^2_{mod})k^2 + A$. Therefore, the slope of this line enables us to determine the difference between the values of σ^2 for the model sample and those for the sample under investigation (22). However, in a number of cases this dependence was found to be nonlinear. According to (17), this could be observed if several chemical elements were located in the same coordination sphere. Model calculations have shown that an analogous effect could be obtained in the case of a non-Gaussian distribution of atoms around the mean position. Such nonlinear dependence could be modeled assuming distances between atoms of the same element to differ by $\Delta R < 0.12$ Å, each having Gaussian distribution (Fig. 4). Hence, by this procedure we have estimated the ΔR values given in Table 2.

EXAFS data obtained for Series A catalysts (Table 2) demonstrate that in agreement with TEM results (*vide supra*) the structure of Pd particles depends upon the nature of the support. Thus, for Pd/SiO_2 the mean Pd–Pd distance exceeds that for pure Pd foil by 0.07 Å, in vacuum, the distances observed in one peak differing by 0.07 Å. In the case of Pd/TiO_2, the Pd–Pd distance is shorter than that in Pd foil by 0.04 Å, the overlapping distances varying by 0.05 Å. For Pd/Al_2O_3 the mean Pd–Pd distance is shorter by 0.1 Å, while ΔR is close to 0.04 Å.

A model assigning change in the Pd–Pd distance to hydride formation would deserve consideration were it not for the results of (23) demonstrating rapid ($t < 20$ sec) disappearance of the β-hydride phase when hydrogen partial pressure is less than 0.01 atm. Hence, in our case, where samples after reduction were evacuated at 673 K (*vide supra*), any hydride presence seems to be rather doubtful.

For all catalysts, CO adsorption (Series B) was accompanied by leveling off the Pd–Pd distances assigned to the surface and those assigned to the bulk of Pd clusters, which

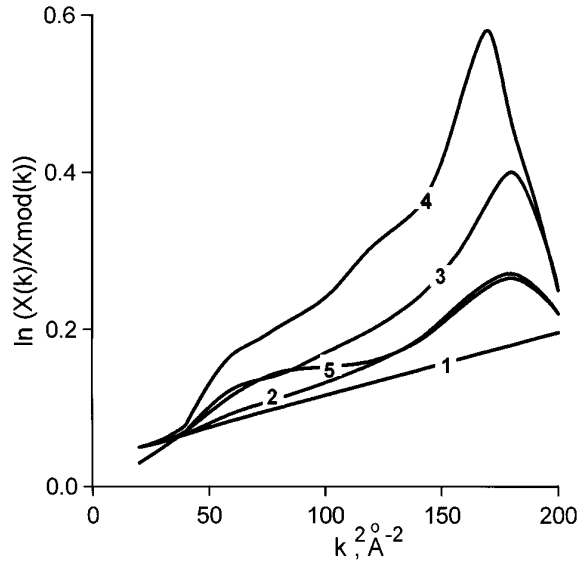

FIG. 4. Dependence of $\ln(\chi(k)/(\chi_{mod}(k))$ vs k^2 for Series A Pd/TiO_2 sample (curve 5) and for double-shell models with $\Delta R = 0.0$ (curve 1), 0.04 (curve 2), 0.08 (curve 3), and 0.12 Å (curve 4) relative to the single-shell model. Pd–Pd mean distance $R_1 = 2.70$ Å. For the single-shell model, $\sigma^2_{mod} = 0.004$ Å^2. For double-shell models, $\sigma^2 = 0.007$ Å^2.

agrees well with the single-crystal data (19). Simultaneously, the Debye factor for Pd/SiO_2 and Pd/TiO_2 increases, while it remains nearly constant for Pd/Al_2O_3 (Table 2). A peak corresponding to the Pd–CO distance was detected for Pd/Al_2O_3 only. The Pd–*L* distance is equal to 1.92 Å, that is, close to the length of Pd–C bonds in the case of terminal Pd carbonyls. The absence of detectable Pd–C peaks for Pd/SiO_2 and Pd/TiO_2 catalysts could be explained by a smaller coverage of the surface by carbon monoxide for Pd/TiO_2 (24) and a somewhat lower dispersion for Pd/SiO_2. In the case of Pd/TiO_2, CO adsorption is not accompanied by variation of the mean Pd–Pd distance, while for other supports this distance approaches that typical for bulk Pd. In general, nondissociative CO adsorption is known to occur without any substantial change of the effective charge of Pd (8). Probably, due to an increase of the degree of Pd atom coordination, the difference between the structure of the surface and that of the bulk disappears. Earlier, a similar phenomenon was observed for CO adsorption on Pt/SiO_2 (11). The increase of the Debye factor after CO adsorption on Pd/SiO_2 and Pd/TiO_2 indicates disordering of the surface layer, as was found in (25, 26).

After treatment of the catalysts with the reaction mixture (Series C), the increase of ΔR (up to 0.08–0.11 Å) and the enhancement of the Debye factor were observed (Table 2), though it is difficult to speak about a real Debye factor at such high values of ΔR. These phenomena indicate strong perturbation of the structure. The character of the structure distortion depends upon the nature of the support and seems to be determined first of all by the adsorption or incorporation of oxygen into the subsurface layer. Thus, for Pd/TiO_2, where the Pd–O peak is not observed, the amount of subsurface oxygen is minimal but the surface is covered by a mixed structure of CO and oxygen (24); the perturbation is manifested by the decrease of Pd–Pd distance, due, probably, to partial charging of the cluster on account of adsorption of electronegative ligands (oxygen). In the case of Pd/SiO_2 and Pd/Al_2O_3, where the surface is covered by CO only (24), the mean Pd–Pd distance increases, indicating probably a rearrangement of the subsurface layer caused by the oxygen incorporation (the peaks attributed to Pd–O distance are observed for both catalysts, relative intensity being higher for Pd/Al_2O_3).

DISCUSSION

The data obtained enable us to draw some conclusions about the influence of the support and reaction media on the structure of Pd clusters. The uniform distribution and the largest sizes of Pd particles on SiO_2 imply that after impregnation, $Pd(OAc)_2$ has been adsorbed on this support uniformly. Pd atoms formed in the course of reduction can further interact only weakly with the surface of SiO_2 and thus they migrate easily to centers of crystallization, whose number is the lowest among the supports investigated. A possible decoration of the Pd particles by a SiOH species obviously will not have any impact on the bulk structure of Pd. Hence, Pd on SiO_2 appears to have a fairly perfect structure, with the Pd–Pd distance in the bulk approaching that of Pd foil.

For other supports, the situation seems to be quite different. It could be presumed that the structure of Pd clusters on TiO_2 and γ-Al_2O_3 is strongly disturbed by the interaction with support. Thus, for Pd/TiO_2 flat clusters of Pd are probably stabilized due to a structural matching with this support. The lowest value of Debye factor for Pd/TiO_2 in vacuum seems to be caused by a decrease of a dynamic increment, thus exhibiting substantial bonding with TiO_2. A dramatic increase of σ^2 for this catalyst under the action of CO indicates the most disordered surface layer among the catalysts investigated. The most probable explanation of this phenomenon is that Pd/TiO_2 has the highest proportion of easily reconstructed faces of the (110) type (28). As could be judged from the retention of Pd lattice contraction even in oxidizing reaction mixtures, the nature of the interaction with this support is unlikely to be associated with the existence of any reduced forms of Ti, since they are known to disappear instantaneously in the presence of oxygen (7).

The absence of any preferential shape for Pd clusters on alumina could indicate a strong interaction of Pd (as well as the starting compound—$Pd(OAc)_2$) with defect centers on the surface of a disordered spinel support. This interaction is also seen from a decreased value of Pd–Pd distance for a sample treated in vacuum. The highest affinity of this sample to oxygen could be attributed to stabilization of the oxidized Pd forms by this support (29).

Hence, the EXAFS data analysis procedure used here for small Pd clusters with nonGaussian distribution of the interatomic distances has been demonstrated to provide physically meaningful results in line with those of other methods.

CONCLUSION

By using TEM and EXAFS, the morphology of Pd clusters on various supports and the influence of carbon monoxide and the reaction mixture $CO + O_2$ on their fine structure have been investigated. The data obtained give evidence of distortion of the surface layer of small clusters, the degree and character of this distortion being dependent upon the nature of support as well as adsorbate. This suggests that variation in the reactivity of adsorbed carbon monoxide may be assigned to disordering of the surface structure of clusters, leading to formation of new active centers.

REFERENCES

1. Ladas, S., Poppa, H., and Boudart, M., *Surf. Sci.* **102**, 151 (1981).
2. Boudart, M., and Rumpf, F., *React. Kinet. Catal. Lett.* **35**, 95 (1987).
3. Rumpf, F., Poppa, H., and Boudart, M., *Langmuir* **4**, 722 (1988).

4. Vorontsov, A. V., and Kasatkina, L. A., *Kinet. Katal.* **21**, 1282 (1980). [In Russian]
5. Miszczenko, Yu. A., Kahniashvili, G. N., Marshakova, E. N., Dulin, D. A., and Gelbshtein, A. I., *Kinet. Katal.* **28**, 619 (1987). [In Russian]
6. Pavlova, S. N., Sazonov, V. A., and Popovskii, V. V., *React. Kinet. Katal. Lett.* **37**, 325 (1988).
7. Poluboyarov, V. A., Dergaleva, G. A., Anufrienko, V. F., Pavlova, S. N., Sazonov, V. A., Popovskii, V. V., and Zenkovets, G. A., *Kinet. Katal.* **30**, 700 (1989). [In Russian]
8. Engel, T., and Ertl, G., *in* "The Chemical Physics of Solid Surfaces and Heterogeneous Catalysis" (D. A. King and D. P. Woodruff, Eds.), Vol. 4, p. 75. Elseiver, Amsterdam, 1982.
9. Boudart, M., *Adv. Catal.* **20**, 153 (1969).
10. Boudart, M., *J. Mol. Catal.* **30**, 27 (1985).
11. Zhang, H., Chen, H., Shen, L.-L., and Sachtler, W. M. H., *J. Catal.* **127**, 213 (1990).
12. Kochubey, D. I., Babanov, Yu. A., Zamaraev, K. I., Vedrinskii, R. V., Kulipanov, G. N., Mazalov, L. N., Skrinskii, A. N., Fedorov, V. K., Helmer, B. Yu., and Shuvaev, A. T., "X-Ray Spectral Method of Structural Study of Amorphous Solids." Nauka (Siberian Branch), Novosibirsk, 1988. [In Russian]
13. Eisenberger, P., and Lengeler, B., *Phys. Rev. B* **22**, 3351 (1980).
14. Chuvilin, A. L., Moroz, B. L., Zaikovskii, V. I., Likholobov, V. A., and Yermakov, Yu. I., *J. Chem. Soc. Chem. Commun.* **1425**, 733 (1985).
15. Anderson, J. "The Structure of Metal Catalysts." Mir, Moscow, 1978.
16. Yang, G. J., Paesler, M. A., and Sayers, D. E., *Phys. Rev. B* **39**, 10342 (1989).
17. Van Zon, J. A. B. D., Koninsberger, D. C., Van't Blik, H. F. J., and Sayers, D. E. J., *J. Chem. Phys.* **82**, 5742 (1985).
18. Chiu, N. S., Bauer, S. H., and Johnson, M. F. L., *J. Catal.* **89**, 226 (1984).
19. Somorjai, G. A., *in* "Annual Review of Physical Chemistry," Vol. 45, p. 721. Annual Reviews, Palo Alto, CA, 1994.
20. Greegor, R. V., and Lyttle, F. W., *J. Catal.* **63**, 476 (1980).
21. Heilmann, P., Heinz, K., and Muller, K., *Surf. Sci.* **83**, 487 (1979).
22. Crescenzi, M., Diociaiuti, M., Picozzi, P., and Santussi, S., *Phys. Rev. B* **34**, 4334 (1986).
23. Boudart, M., and Hwang, H. S., *J. Catal.* **39**, 44 (1975).
24. Pavlova, S. N., Sadykov, V. A., Bulgakov, N. N., Razdobarov, V. A., and Paukshtis, E. A., *J. Catal.* **161**, 517 (1996).
25. Yuszczyk, W., Karpinski, Z., Ratajczykova, I., Stanasiuk, Z., and Zielinski, J., *J. Catal.* **120**, 68 (1989).
26. Bart, J. C. J., and Vlaic, G., *Adv. Catal.* **35**, 1 (1987).
27. Hu, P., de la Garza, M., Raval, R., and King, D. A., *Surf. Sci.* **249**, 1 (1991).
28. Gaussman, A., and Kruse, N., *Catal. Lett.* **35**, 95 (1987).
29. Sass, A. S., Shvets, V. A., Savelyeva, G. A., Popova, N. M., and Kazanskii, V. B., *Kinet. Katal.* **23**, 1153 (1982). [In Russian]